RESEARCH ARTICLE

Evaluation of NiFe Bifunctional Electrocatalysts for Rechargeable Sodium-Ion-Based Seawater Batteries

Lakshmi Narayana Manickavasagam[1,2] | Rohan Murugavel[1] | Anubala Singaravelu Kumar[1] | Nitin Muralidharan[1,2]

[1]Department of Chemical Engineering, Indian Institute of Technology Madras, Chennai, Tamil Nadu, India | [2]Centre for Resource Efficiency, Recyclability, and Circularity in Energy Transition, School of Sustainability, Indian Institute of Technology Madras, Chennai, Tamil Nadu, India

Correspondence: Nitin Muralidharan (muralidharan@iitm.ac.in)

Received: 15 February 2026 | **Revised:** 13 July 2026 | **Accepted:** 25 July 2026

Keywords: bifunctional electrocatalyst | energy storage | layered double hydroxides | seawater battery | sodium ion

ABSTRACT

Rechargeable sodium-based seawater batteries (SWBs) that store energy in the form of metallic Na at the anode require cathodes laden with bifunctional electrocatalysts that can efficiently perform the otherwise kinetically sluggish oxygen evolution (OER) and reduction reactions (ORR). Here, we report the systematic evaluation of NiFe layered double hydroxides (NiFe-LDHs) as suitable bifunctional electrocatalysts for use in rechargeable SWBs. NiFe-LDHs with various Ni/Fe ratios were synthesized using a hydrothermal approach to ensure spherical particle morphologies comprising of flowerlike nanosheets pattern on the surface with high surface area of ~63 m^2/g. The electrocatalytic activities and operational stabilities of these synthesized catalysts were evaluated using linear sweep voltammetry and chronopotentiometry in both simulated seawater and natural seawater. The LDH catalysts evaluated in our study showed comparable catalytic behavior in simulated seawater, whereas in natural seawater, performances drastically varied. Additionally, the best performing catalyst was tested in a dual compartment Na seawater cell, demonstrating successful sequential OER and ORR operation in natural seawater. Overall, this study highlights the potential of NiFe-LDH bifunctional electrocatalysts for rechargeable Na-based seawater batteries and elucidates the feasibility and design parameters of such catalysts for effective OER and ORR activity in conditions employing natural seawater in SWBs.

1 | Introduction

Battery energy storage systems (BESS) are essential to store and deliver electrical energy on demand as well as offset the energy fluctuations caused by integration of renewables to the power grid, which are, generally, intermittent and weather dependant [1, 2]. Li-ion batteries are ideal BESS candidates as they deliver high energy density and long cycle life [3–5]; however, the supply chain constraints and limited availability of critical materials (Li, Ni, Co) in combination with the rapidly increasing demand for electric vehicles and portable devices [5–7] have thrust upon us the need to explore other low-cost and earth abundant alternatives to Li-ion systems [8, 9].

In this quest, dual compartment rechargeable seawater batteries (SWBs) that utilize Na^+ ions from seawater [10, 11] to store and deliver energy on demand has been gaining traction in the R&D space as a viable alternative. A schematic representation of such a system is shown in Figure 1a. The rechargeable SWB consist of an anode and a cathode compartment separated by a membrane/plate/separator which forms the linchpin of this device. The anode compartment comprises of an organic electrolyte, while the cathode compartment enables the use of aqueous electrolytes including natural seawater. The membrane/plate/separator that separates these two compartments needs to conduct only Na^+ ions through while being inert to both organic and aqueous electrolytes on either side. Over the past decade, ceramic sodium superionic conductors (NASICON) solid electrolytes have been actively explored in the field of solid state batteries owing to their high Na^+ conductivities (~10^{-3} to 10^{-4} Scm^{-1} at room temperature) and excellent structural stabilities [12, 13]. NASICON solid electrolyte ceramics are ideal for use in these rechargeable seawater batteries,

and they have been widely reported to show excellent stabilities in both organic and aqueous electrolytes [14–16]. Energy in these SWB devices is usually stored in the form of Na metal plated at the anode [17, 18]. While the Na^+ ions shuttle to and fro between the anode and cathode compartments through the NASICON solid electrolyte, oxygen evolution (charging) and oxygen reduction (discharging) reactions occur at the cathode. The half-cell and overall reactions are as follows:

$$\text{Anode: } Na^+ + e^- \leftrightarrow Na \qquad E^o = -2.25V \text{ versus RHE} \tag{1}$$

$$\text{Cathode: } O_2 + 2H_2O + 4e^- \leftrightarrow 4OH^- \qquad E^o = 1.23V \text{ versus RHE} \tag{2}$$

$$\text{Overall reaction: } 4Na + 2H_2O + O_2 \leftrightarrow 4NaOH \qquad E^o = 3.48V \text{ versus } Na/Na^+ \tag{3}$$

These OER and ORR reactions have sluggish rates, and therefore, it is imperative that a bifunctional catalyst that is active for both oxygen evolution and reduction reactions is required to obtain improved performance of the SWB battery.

In the field of electrocatalysis, Pt/C and RuO_2/IrO_2 are the state of art for ORR and OER, respectively. However, their high cost and low activity for the simultaneous forward and reverse reactions restrict their application towards such large-scale energy storage systems like the SWBs [19]. Alternatively, transition metal-based layered double hydroxides are considered a comparable low-cost alternative to noble metal based electrocatalysts for ORR and OER activities [20–23]. In this regard, NiFe layered double hydroxides (NiFe-LDH) is a widely explored bifunctional transition metal based electrocatalyst that boast comparable lower cost, tunable chemical compositions and good catalytic activity in alkaline environments [24–27] and also seawater [28, 29].

Here, in this study, the potential of NiFe layered double hydroxides (NiFe-LDHs) as electrocatalyst for rechargeable Na-based seawater battery has been systematically investigated. NiFe-LDHs with various Ni/Fe ratio were synthesized using hydrothermal process to achieve compact spherical morphologies with flower-like surface LDH [24, 30]. The electrocatalytic activity toward sequential OER and ORR were investigated in alkaline simulated seawater [28, 31, 32] (which is what is usually reported in literature) as well as natural unmodified seawater to elucidate the performance in practical on-field conditions. Additionally, the long duration stabilities of the prepared NiFe-LDHs were evaluated, following which a rechargeable Na seawater battery was assembled and tested using the best performing catalyst composition. Broadly, through this study we highlight the potential of NiFe-LDHs as a cost-effective and stable electrocatalyst for sequential ORR and OER activities in rechargeable Na based seawater batteries.

2 | Results and Discussion

The crystal structure of the NiFe-LDHs synthesized using the hydrothermal process was characterized using X-ray diffraction technique (XRD). Figure 1b shows the diffraction pattern of the prepared LDHs with various Ni/Fe ratios. The diffractograms revealed that $Ni(OH)_2$ and FeOOH crystallized in R-3 m and I 4/m space groups. The prepared NiFe-LDHs has diffraction pattern similar to that of $Ni_{0.75}Fe_{0.25}(CO_3)_{0.125}(OH)_2.0.38H_2O$ [24]. The major diffraction peaks of the NiFe-LDHs at 11.7°, 23.5°, 34.6°, 39.0°, and 59.9° correspond to the (003), (006), (012), (015) and (110) planes. With increase in Fe content, new peaks emerge in the diffraction pattern due to the presence of β-FeOOH phase. The peaks at 17.0°, 27.1°, 35.5°, and 56.5° correspond to the (200), (130), (211), and (251) crystal planes of β-FeOOH phase. β-FeOOH phase in NiFe-LDH has been reported previously to increase the electrocatalytic activity, through the formation of β-Ni(Fe)OOH phase [33]. The observed XRD patterns are comparable to standard patterns thus confirming the formation of crystalline NiFe-LDHs through our hydrothermal process. As surface area is an important parameter for catalysts, BET surface area analysis was performed, and Figure 1c shows the comparison of BET isotherms of hydrothermal synthesized NiFe-1:2 and commercially procured 20% Pt/C as a control. The figure inset shows the comparison of BET surface area of the same. N_2 adsorption/desorption curve of the NiFe-1:2 shows characteristics of type IV isotherm with H3 hysteresis loop [34] indicating that NiFe-1:2 is mesoporous and the BET surface area of the NiFe-1:2 was calculated to be ~63 m^2/g which is twice as high as that of commercially procured 20% Pt/C (38 m^2/g).

Morphological characterization of the prepared NiFe-LDH was performed using Scanning Electron Microscopy (SEM). The electron micrographs shown in Figure 1d,e reveal that the hydrothermal synthesized NiFe-LDH exhibit spherical morphologies and the spheres are observed to comprise interconnected nanosheets of NiFe-LDH. The presence of these interconnected nanosheets is expected to increase the number of electrocatalytically active sites resulting from the exposed large surface area as evidenced through the BET surface area analysis. Further, to analyze the distribution of metal ions, EDS mapping was performed. The elemental mapping of the NiFe-LDH sphere shown in Figure 1f reveals uniform distribution of the Ni, Fe, and O atoms across the sphere, thus confirming no segregation of the metal atoms. Further investigation of the surface of NiFe-LDH was carried out using transmission electron microscopy (TEM). Figure 1g shows the TEM image which highlights the well-defined spherical particles of the hydrothermal synthesized NiFe-LDH made of clusters of nanosheets. Further, the selected area electron diffraction pattern shown in Figure 1h depicts 3 well defined concentric rings, corresponding to the (012), (015), and (110) planes, confirming high crystallinity of the synthesized NiFe-LDH.

Following the material and morphological characterizations, the NiFe-LDH catalysts were subjected to electrochemical performance assessment in controlled 3-electrode setups similar to those reported widely in literature. The electrocatalytic performance of the NiFe-LDHs were investigated by coating the catalysts on carbon cloth and subjecting them to linear sweep voltammetry (LSV) tests in alkaline simulated seawater (3.5% NaCl in 1M KOH, widely reported in literature) in a three-electrode system as shown in Figure 2a. The electrocatalytic performance of bare carbon cloth and commercial prevalent catalysts; for example, 20% Pt/C, and IrO_2 were also measured as controls. LSV tests were

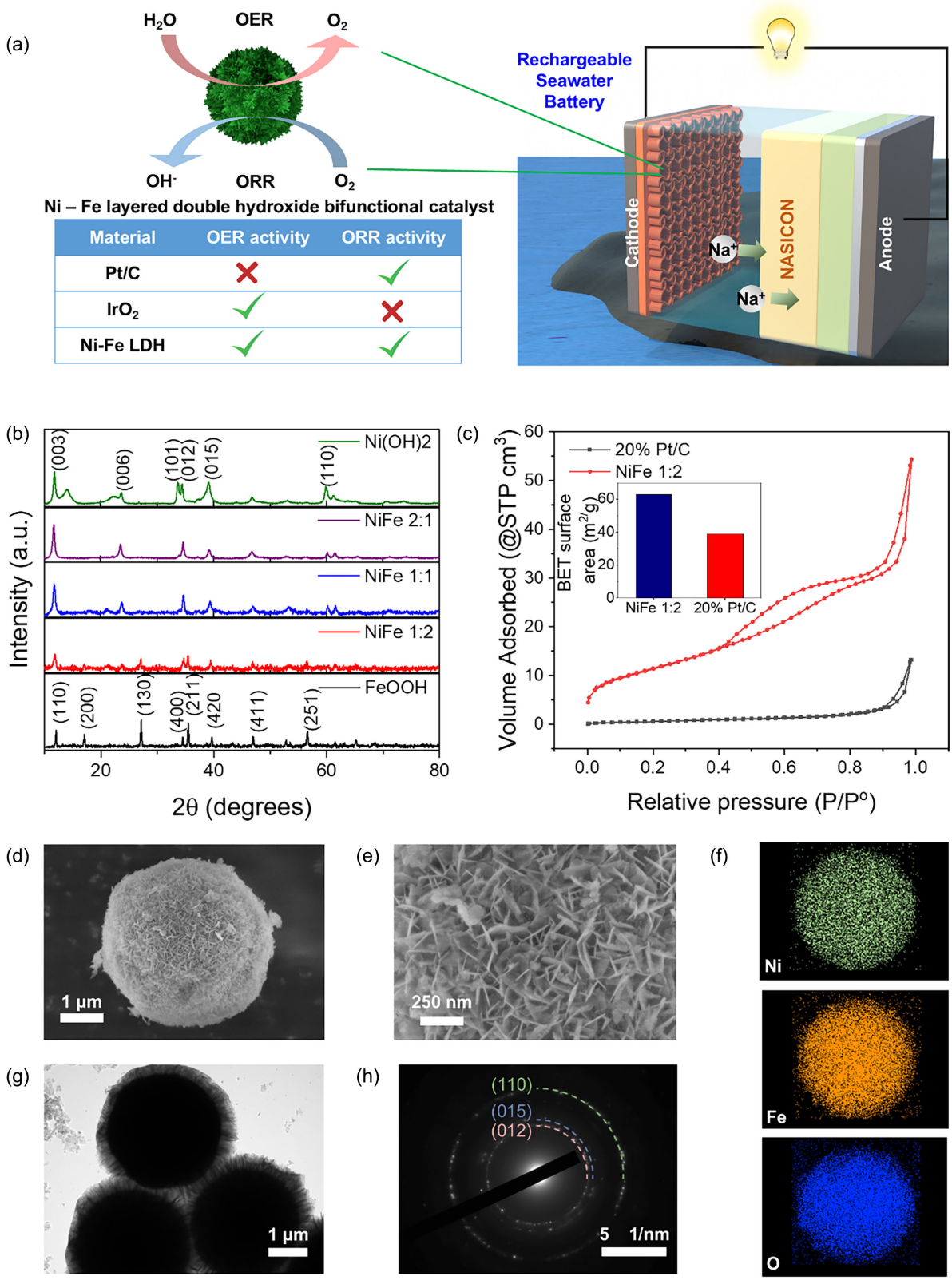

FIGURE 1 | (a) Schematic representation of a rechargeable Na-based seawater battery with the NiFe-LDH electrocatalyst. (b) X-ray diffraction pattern of the synthesized LDHs. (c) comparison of BET isotherms of NiFe 1:2 and 20%Pt/C (inset comparison of surface area calculated). SEM images illustrating (d) spherical morphology. (e) Nanosheets of LDH. (f) EDS elemental mapping of NiFe-LDH. (g) TEM images. (h) SAED pattern of the synthesized NiFe-LDH.

conducted to analyze the electrocatalytic activity of the prepared LDHs toward both oxygen evolution and oxygen reduction reaction in sequential manner to explore the bifunctional nature of the catalytic activity (Figure 2b). Comparison of the overpotential (η) at 5 mA/cm^2 (Figure 2c) revealed that OER overpotentials for the prepared LDHs NiFe 2:1 (η_{OER} – 280 mV), NiFe 1:1 (η_{OER} – 297 mV),

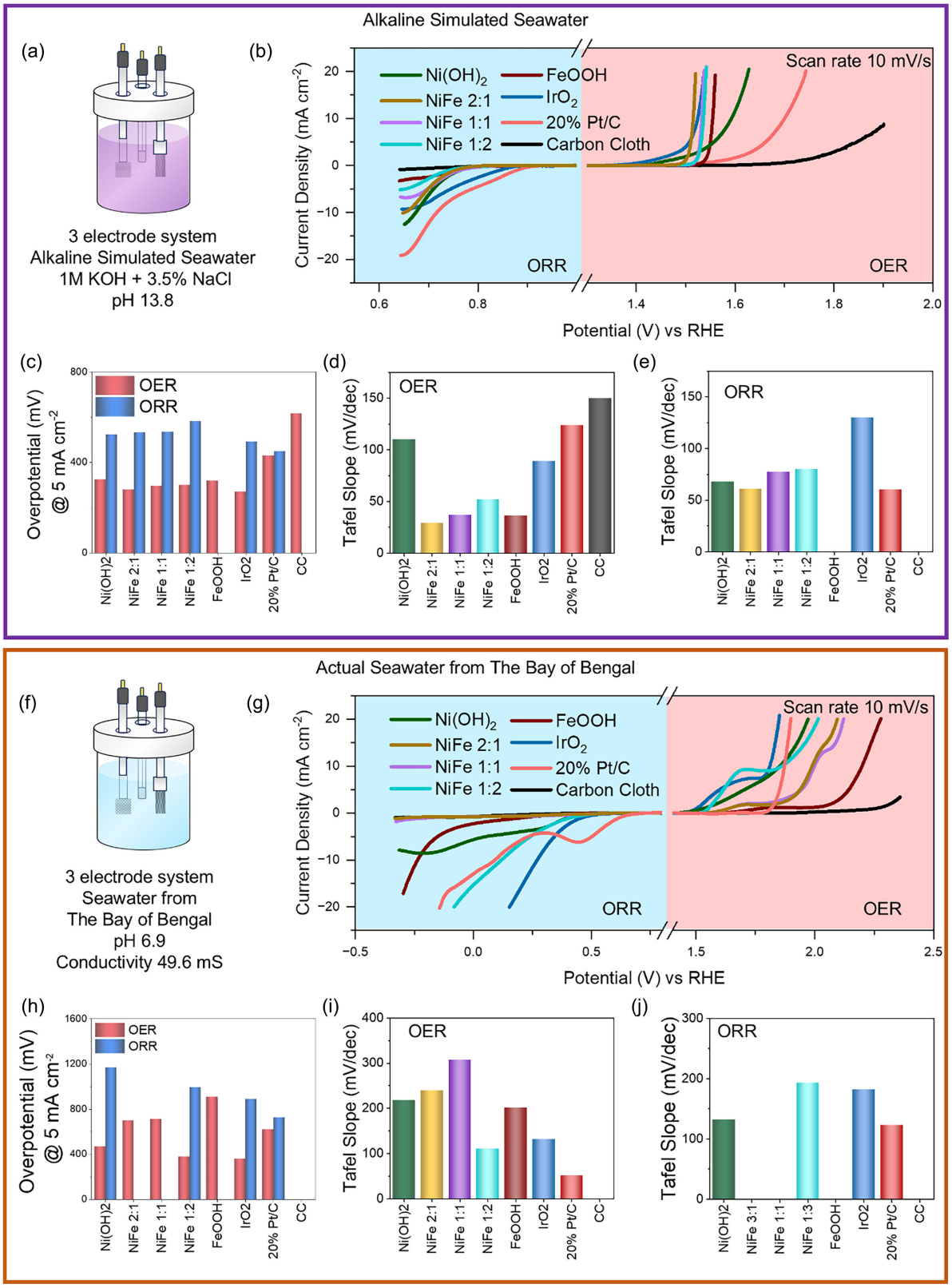

FIGURE 2 | (a) Schematic representation of a three-electrode setup. (b) Comparison of LSVs of different electrodes. Tafel slopes of (c) OER and (d) ORR. (e) Comparison of overpotential at 5 mA/cm^2 in 1M KOH + 3.5% NaCl solution. (f) Schematic representation of three-electrode setup. (g) Comparison of LSVs of different electrodes. Tafel slopes of (h) OER and (i) ORR. (j) Comparison of overpotential at 5 mA/cm^2 in seawater from the Bay of Bengal.

and NiFe 1:2 (η_{OER} – 300 mV) were lesser than that of $Ni(OH)_2$ (η_{OER} – 325 mV), and FeOOH (η_{OER} – 318 mV). The OER activity of the prepared NiFe-LDHs were comparable to that of state of art oxygen evolution catalyst IrO_2 (η_{OER} – 270 mV). However, the ORR overpotential of the LDHs NiFe 2:1 (η_{ORR} – 533 mV), NiFe 1:1 (η_{ORR} – 534 mV), and NiFe 1:2 (η_{ORR} – 582 mV) were significantly

higher than that of state of art oxygen reduction electrocatalyst 20% Pt/C (450 mV). The control test using carbon cloth showed very high overpotential for OER (η_{OER} – 616 mV) and no activity for ORR. Further, the reaction kinetics of the prepared electrodes were analyzed using Tafel plots obtained from the LSV tests. Figure 2d,e shows the comparison of Tafel slopes for OER and ORR reactions in alkaline simulated seawater. The prepared NiFe-LDHs NiFe 2:1 (29 mV/dec), NiFe 1:1 (37 mV/dec), and NiFe 1:2 (52 mV/dec) exhibited lower Tafel slopes than $Ni(OH)_2$ (110 mV/dec), IrO2 (89 mV/dec) indicating that the NiFe-LDHs have faster charge transfer and kinetic reaction rate for oxygen evolution reaction. Similarly, for the oxygen reduction reaction the prepared NiFe-LDHs, NiFe 2:1 (61 mV/dec), NiFe 1:1 (77 mV/dec), and NiFe 1:2 (80 mV/dec) exhibit comparable Tafel slopes to that of 20% Pt/C (60 mV/dec). The electrocatalytic activity is comparable to other OER/ORR bifunctional electrocatalyst (Table S1) [26, 35–39]. These results confirmed that the prepared NiFe-LDHs showed good electrocatalytic activity toward both OER and ORR highlighting their excellent bifunctional catalytic activity.

Though the testing of the LDHs in simulated solutions with known concentration of ions provides us information on the catalytic behavior, the end goal of the synthesized bifunctional catalysts (NiFe-LDH in this case) is to be used as electrocatalysts in rechargeable Na based seawater batteries utilizing natural unmodified seawater akin to on field conditions. Therefore, the electrocatalytic activity of the NiFe-LDHs were investigated in natural unmodified seawater collected from the Bay of Bengal (GPS Coordinates, 13.047509, 80.283310; closest city, Chennai, India near Indian Ocean). The linear sweep voltammetry (Figure 2g) were performed in a three-electrode system similar to that used previously for alkaline simulated seawater as shown in Figure 2f. The collected natural seawater was used directly without any pretreatment (pH ~ 7). Comparison of the overpotential at 5 mA/cm^2 (Figure 2h) revealed that, out of the various compositions of NiFe-LDHs prepared, NiFe 1:2 had lower overpotential for OER (η_{OER} – 380 mv) which is similar to that of IrO_2 (η_{OER} – 360 mV). For the oxygen reduction reactions, $Ni(OH)_2$ showed very high overpotentials, FeOOH, NiFe 2:1 and NiFe 1:1 showed no activity. However, NiFe 1:2 (η_{ORR} – 990 mV) showed measurable catalytic activity which is comparable to that of 20% Pt/C (η_{ORR} – 725 mV). Further the Tafel slopes for NiFe 1:2 (η_{OER} – 111 mV/dec and η_{ORR} – 193 mV/dec) was comparable to that of IrO_2 (η_{ORR} – 132 mV) and 20% Pt/C (η_{ORR} – 123 mV/dec). The exact reason for this trend requires further investigations and could be a result of interference from other ions/salts present in natural unmodified seawater. Nevertheless, in light of the trends obtained, the NiFe layered double hydroxide with Ni/Fe ratio 1:2 was selected for further evaluations.

The stabilities of the synthesized NiFe-LDH catalysts were evaluated using chronopotentiometric tests in a two electrode symmetric cell set up in which oxygen evolution reaction takes place at the anode and oxygen reduction reaction takes place at the cathode, thus simultaneously ORR and OER activity of the bifunctional catalyst were tested. The long-term stability of NiFe 1:2 electrocatalyst was tested in alkaline simulated seawater as shown in Figure 3a at a current density of 0.1 mA/cm^2. Comparatively, commercially procured control: 20% Pt/C showed higher potential till 50 h of operation following which the potential dropped significantly, possibly due to the activation of the catalyst, whereas NiFe 1:2 showed stable voltage for 100 h of continuous operation and the potential throughout was similar to the potential of 20% Pt/C after 50 h. The electron micrographs Figure 3a inset (i), (ii), and (iii) show that the catalysts in both anode and cathode showed no significant degradation or cracking, highlighting the excellent structural and morphological stabilities of the NiFe-LDH electrocatalysts for long duration applications. Further, chemical stability of the catalyst after 100 h of operation was analyzed using XPS. The XPS spectrum of Ni 2p of both the cathode Figure 3c and anode Figure 3d after 100 h of continuous operation showed intense peaks around 855 eV and 873 eV which correspond to the Ni $2p_{3/2}$ and Ni $2p_{1/2}$ j–j coupling of Ni^{2+} oxidation state, respectively, and the peaks at 861 and 879 eV are satellite peaks. The Fe 2p spectrum of the cathode was deconvoluted into four peaks as shown in Figure 3c, of which the peaks at 711 and 724 eV correspond to the Fe $2p_{3/2}$ and Fe $2p_{1/2}$ j–j coupling of the Fe^{3+} oxidation state, and the peaks at 719 and 730 eV are satellite peaks. The Fe 2p spectrum of the anode (Figure 3d) after 100 h of continuous operation was deconvoluted into three peaks, Fe $2p_{3/2}$ peak at 711 eV, satellite peak at 717 eV, and a broad peak at 725 eV. The O 1s spectra of both the anode and cathode were deconvoluted into three peaks around 530.6, 532, and 535 eV as shown in Figure 3c,d. The intense peak at 530.6 eV corresponds to the M–OH oxygen present in the sample confirming that the material has not undergone any significant structural change at the surface where the catalytic reactions occur. The peak around 532 eV corresponds to adsorbed water molecules present in the sample, and the broad peak at 535 eV correspond to Na KLL auger electrons.

The chronopotentiometric stability test confirmed that the material was stable for both oxygen evolution reaction (anode) and oxygen reduction reaction (cathode) for 100 h of continuous operation, however, when used in rechargeable batteries the material would undergo repeated charging and discharging reactions in a cyclic manner. Therefore, to understand the cycling stability, 50 cycles of chronopotentiometry with 1 h of positive current and 1 h of negative current was performed mimicking a galvanostatic charge discharge test done on a rechargeable battery. Figure 3e shows that NiFe 1:2 initially gets activated showing comparatively lower potential than 20% Pt/C between 10 and 40 h; however, the activity gradually stabilizes after 20 cycles, whereas 20% Pt/C progressively gets activated and exhibits lower overpotential on subsequent cycles. The XPS spectra were collected on the cycled electrodes as well and are as shown in Figure 3f. The Ni 2p spectra was same as previous and was deconvoluted with four peaks around 855, 861, 873, and 878 eV. The Fe 2p spectra was deconvoluted to four peaks as well with peaks at 711, 716, 724.8, and 729.6 eV. The XPS pattern confirmed that Nickel and Iron have the same 2+ and 3+ oxidation states after cycling stability test as well. The O 1s spectra showed three distinct peaks at 530.7, 532, and 535 eV corresponding to M–OH, adsorbed water molecules, and Na KLL auger peak. Thus, confirming that the material is stable under cycling conditions as well.

Next, the same electrochemical stability tests were performed with natural unmodified seawater to understand the robustness of our NiFe-LDH catalysts for potential use in Na seawater battery. The chronopotentiometric stability tests were performed in a 2-electrode setup as shown in Figure 4b. Figure 4a depicts that NiFe 1:2 had a constant overpotential throughout the 100 h of

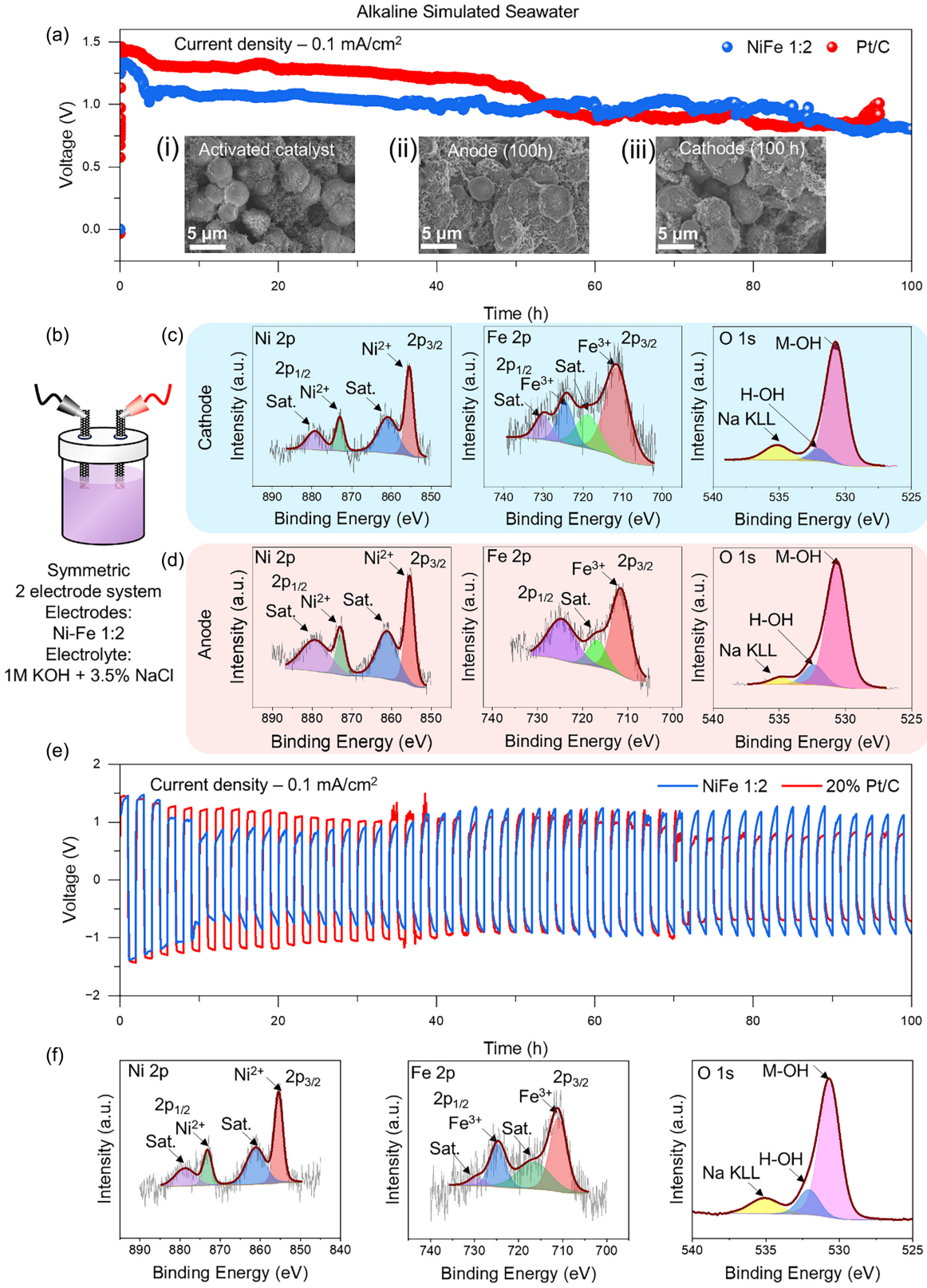

FIGURE 3 | (a) Comparison of chronopotentiometric stability of NiFe 1:2 and 20% Pt/C in alkaline simulated seawater. (b) Experimental setup; post-chronopotentiometry XPS of NiFe 1:2. (c) Cathode. (d) Anode. (e) Galvanostatic charge discharge profile of NiFe 1:2 and 20% Pt/C in alkaline simulated seawater. (f) Post-GCD XPS of NiFe 1:2 electrode.

continuous operation. However, 20% Pt/C initially showed low overpotential, but after 60 h the overpotential increased and stabilized around 1.5 V. The overpotential of the system with NiFe 1:2 was higher than that of 20% Pt/C as expected. Figure 4c shows the optical image of the tested cathode and anode which revealed deposits of thick layer of white powder on the cathode, while that

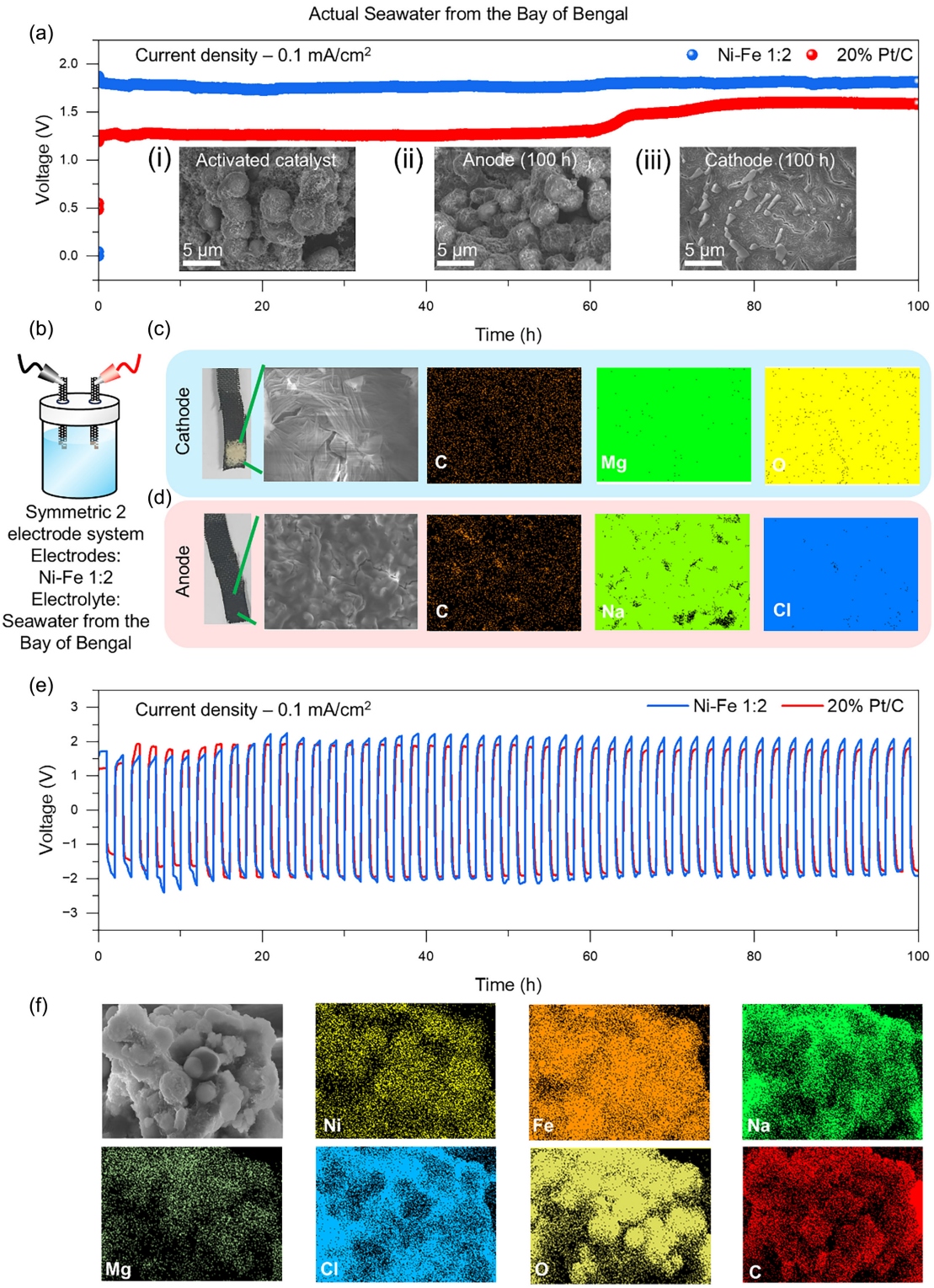

FIGURE 4 | (a) Comparison of chronopotentiometric stability of NiFe 1:2 and 20% Pt/C in natural unmodified seawater collected from the Bay of Bengal. (b) Experimental set up; postchronopotentiometry EDS mapping. (c) Cathode. (d) Anode. (e) Galvanostatic charge discharge profile of NiFe 1:2 and 20% Pt/C in actual seawater from the Bay of Bengal. (f) Post-GCD SEM/EDS of NiFe 1:2 electrode.

of anode did not show any deposits. Electron micrographs and EDS mapping (Figure 4d) were performed on the tested cathode and anode to analyze the structural stability of the electrocatalyst and composition of the deposits. The SEM image of the anode shows that the catalyst is intact; however, it is covered by deposits and the SEM image of the cathode shows thick continuous deposit completely covering the cathode material. The EDS mapping of the cathode revealed that the deposit is mostly made up of Mg and O. The surface of the anode revealed presence of Na and Cl expected on the surface of the catalyst particles. Further, cycling stability of the electrocatalysts in natural seawater was analyzed in a similar manner to that tested for alkaline simulated

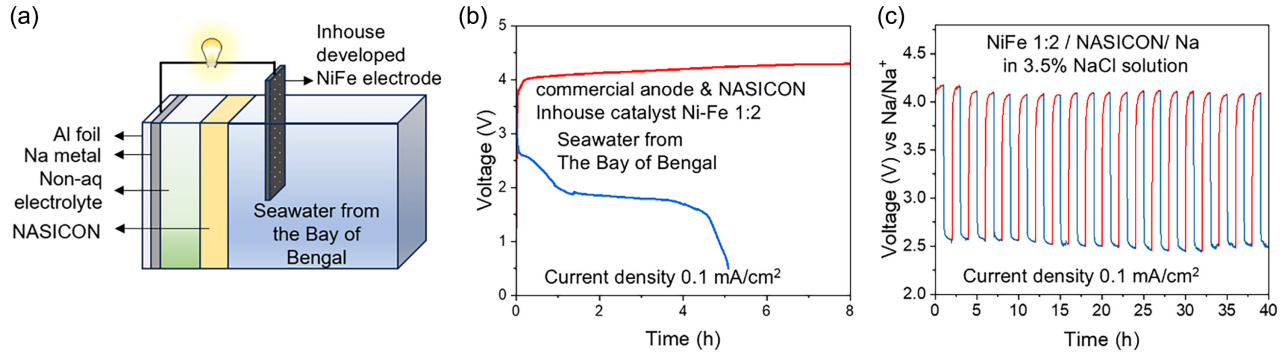

FIGURE 5 | (a) Schematic representation of assembled seawater cell; (b) galvanostatic charge discharge of the assembled seawater cell with inhouse developed NiFe 1:2 electrocatalyst in actual seawater collected from the Bay of Bengal; and (c) cycling stability of NiFe 1:2 in 3.5% NaCl solution.

seawater. As shown in Figure 4e, both NiFe-LDH and 20% Pt/C exhibited similar profiles during charging and discharging with 20% Pt/C exhibiting slightly lower overpotential. This suggests that NiFe-LDH and 20% Pt/C have comparable activity on long time cycling at 0.1 mA/cm^2, and hence NiFe-LDH can be used as a viable alternative. The EDS mapping of the cycled electrode (Figure 4f) revealed deposits of chlorides and oxides of Na and Mg, which are the predominant cations present in the seawater (Table S2), on the surface of the NiFe-LDH catalyst. Similar deposits were found on the 20% Pt/C as well. These salt deposits can grow on continuous operation and eventually block the OER/ORR sites. However, the growth of such deposits can be prevented by employing a continuous flow system, where the flowing solution would remove the salt deposits over the catalysts or feeding demineralized water or low concentration solutions to dissolve the deposits [40]. Techniques similar to descaling of membranes can also be used to remove deposits over catalyst. Ultrasound creating acoustic cavitation can be used to remove the thick salt deposits [41, 42].

To demonstrate the potential of NiFe LDH as an electrocatalyst in an Na-based rechargeable seawater battery, as shown in Figure 5a, a seawater cell with anode compartment (procured from 4toONE) consisting of Al current collector, separator soaked with organic electrolyte and NASICON solid electrolyte ceramic disc was assembled with the in house developed NiFe 1:2 electrocatalyst immersed in natural seawater. The assembled cell had an OCV of 1.5 V, and Figure 5b shows the charge discharge profile of the assembled seawater cell. The cell was charged continuously with a current density of 0.1 mA/cm^2 for 8 h, mimicking the solar cycling with sunlight availability between 8 am and 4 pm in India (assuming conditions where solar charging is employed for potential Behind the meter storage applications). The charging voltage was close to 4.2 V and was stable throughout the charging. However, during discharging, the voltage dropped from 3 V in the 1st hour and was stable at 2 V for 3.5 h before dropping to lower cut-off voltage. The energy delivered by the SWB in this specific configuration was determined to be 29.5 mWh (prototype cell which requires further optimization). Nevertheless, the NiFe catalyst was successfully employed in a rechargeable SWB battery with a prototype lab scale configuration where successful ORR and OER activity was observed highlighting the potential of these bifunctional catalysts. In addition, the cycling stability of NiFe catalyst in seawater battery was tested in simulated seawater (3.5% NaCl), at current density 0.1 mA/cm^2, with 1 h of charging and discharging duration. The assembled cell showed stable cycling for 20 cycles and delivered a constant discharge voltage of 2.6 V (Figure 5c).

3 | Conclusion

To realize practical, field deployable rechargeable Na-based seawater battery systems, bifunctional electrocatalysts that are stable in natural seawater are vital. Here, we have systematically evaluated NiFe-LDHs as a stable electrocatalysts for rechargeable seawater batteries using natural unmodified seawater. Using hydrothermal synthesis NiFe-LDHs of various Ni/Fe ratios were successfully synthesized and characterized of compositional homogeneity and crystallographic phase purity. The synthesized LDHs exhibited spherical morphologies comprising of flower-like surface nanosheets of Ni/Fe boasting a BET surface area of ~63 m^2/g. Electrochemical performance evaluation of these materials were performed in alkaline simulated seawater and in natural seawater to investigate the bifunctional electrocatalytic activity in controlled conditions and in the presence of other ions in natural seawater (mimicking on field conditions). The synthesized LDHs showed comparable electrocatalytic activity in alkaline simulated seawater, however from our evaluations, only the NiFe 1:2 composition showed appreciable activity in natural unmodified seawater. The Tafel slopes and overpotential @ 5 mA/cm^2 of NiFe 1:2 for OER and ORR in seawater were comparable to that of state-of-the-art electrocatalysts, 20% Pt/C and IrO_2, which were used as controls in our study. Further, stability studies in alkaline simulated seawater revealed that the NiFe-LDH was stable and morphologically intact even after 100 h of continuous operation and cyclic operation. However, in actual seawater, though NiFe-LDH had a constant potential (~1.7 V), it was significantly higher than that of 20% Pt/C (~1.3 V). Moreover, the electrodes were covered with thick salt deposits which could completely shield the active sites. The EDS mapping of the tested electrodes revealed that the deposits were salts of Na and Mg ions predominantly. Further studies are required in order to develop solutions to mitigate salt deposition at the cathode side during operation of the seawater battery in on field conditions. Furthermore, we assembled a rechargeable seawater battery (2 V) performed charge discharge tests to demonstrate the application of the prepared NiFe-LDH as a viable electrocatalyst to perform

sequential ORR and OER reactions. Broadly, our work highlights the potential of NiFe-LDH as a low-cost alternative to noble metal based electrocatalysts for rechargeable seawater battery, owing to its sequential ORR and OER electrocatalytic activities.

4 | Experimental Section

4.1 | Synthesis of NiFe Layered Double Hydroxide Particles

NiFe LDHs of various stoichiometric ratios (1:0, 2:1, 1:1, 1:2, and 0:1) were synthesized using a one-pot hydrothermal method. Stoichiometric amounts of $Ni(NO_3)_2{\cdot}6H_2O$ (99%, Sisco Research Laboratories. Pvt. Ltd), and $Fe(NO_3)_3{\cdot}9H_2O$ (98%, Sisco Research Laboratories. Pvt. Ltd) were dissolved in 50 mL of DI water. 130 mmol of urea (99%, Thermo Fisher Scientific India Pvt. Ltd) and 27 mmol of NH_4F (99%, Spectrochem Pvt. Ltd) were added to the mixture at room temperature to obtain a uniform solution. The solution was made to 100 mL, then transferred to a 200 mL Teflon-lined autoclave reactor which was then kept at 105 °C for 12 h and naturally cooled. The solution was then centrifuged to obtain NiFe LDH powders, which were then washed with DI water and with ethanol, sequentially. The powders were then dried under vacuum at 60 °C.

4.2 | Fabrication of Electrodes

NiFe-LDHs, Super P carbon (The Electrode Store (TES)), PVDF (Solaf, TES), and carbon cloth (TES) were dried under vacuum at 60 °C, overnight. Electrode ink was prepared using 8:1:1 ratio of NiFe-LDHs (electrocatalyst):Super P (conducting carbon):PVDF (binder), with n-methyl-2-pyrrolidone (Labkarts. Pvt. Ltd) as solvent respectively. The ink was sonicated for 30 min to obtain a uniform solution following which it was dropcast over carbon cloth to obtain a final loading of 2 mg/cm^2. 20% Pt/C (TES) and IrO_2 (TES) were used as controls.

4.3 | Electrochemical Characterization

Electrochemical measurements were performed using Autolab potentiostats/galvanostats (M204 and portable potentiostat), in a three electrode setup, with the as prepared electrodes as working electrode, Pt mesh (1 cm × 1 cm) as counter electrode and Ag/AgCl in 3 M KCl as reference electrode. The electrodes were tested in 1M KOH + 3.5% NaCl solution and natural unmodified seawater collected from the Bay of Bengal. Electrochemical Impedance Spectroscopy (EIS) measurements were performed in the frequency range of 100 kHz to 1 Hz to identify the solution resistance for IR drop correction. The electrodes were activated using 10 cycles of cyclic voltammetry (CV) at a scan rate of 50 mV/s in the respective electrolytes before performing the electrochemical tests as shown in Figures S2 and S3. Linear sweep voltammetry studies were performed at a scan rate of 10 mV/s and the obtained data were 80% IR corrected. The potentials were converted to RHE using the equation $E_{RHE} = E_{Ag/AgCl\ in\ 3M\ KCl} + 0.0591 \times pH + 0.210$. The pH for 1 M KOH + 3.5% NaCl was 13.8 and for natural seawater was 6.9. Neware battery cyclers were used to perform the stability tests and galvanostatic charge discharge cycle of seawater cell and Autolab Potentiostat/Galvanostat was used to perform the cycling stability tests in simulated seawater (3.5% NaCl). The dual compartment Na Seawater battery was assembled using 4ToONE seawater test jig. 2464 coin cells obtained from 4ToONE containing Al current collector, separator soaked with non-aqueous electrolyte, and NASICON solid electrolyte, was used as the anode compartment. Natural unmodified seawater collected from the Bay of Bengal was used without any pre-treatments in the cathode compartment.

4.4 | Material Characterization

The as synthesized NiFe-LDH and the fabricated electrodes (pristine and tested) were characterized using techniques such as X-ray diffraction (XRD), scanning electron microscopy (SEM), energy-dispersive spectroscopy (EDS), transmission electron microscopy (TEM), selected area electron diffraction (SAED), Brunauer–Emmett–Teller (BET) surface area analysis, and X-ray photoelectron spectroscopy (XPS). X-ray diffraction measurements were performed using Thermo Scientific ARL EQUINOX 3000 at 40 KV 30 mA conditions. The XRD data was collected at under simultaneous acquisition at room temperature using Cu-Kα radiation. SEM and EDS measurements were performed using Hitachi S-4800 employing Tungsten cold field emission gun. TEM images and SAED pattern were collected using JEOL JEM 3010 transmission electron microscope. TEM sample was prepared by dispersing the catalyst powder in ethanol and drop casting it over carbon coated copper grid. BET measurements were performed using Anton Paar Nova 600. XPS measurements were performed using Thermo Scientific K-Alpha XPS system with Al-Kα radiation. Inductively coupled plasma–mass spectroscopy measurements on seawater and NiFe LDH powder were performed using NexION 1000–Perkin Elemer with Ar Plasma. The seawater used in ICP-MS measurements was filtered using a 0.45 µm syringe filter to ensure removal of any particulate matter.

Author Contributions

Lakshmi Narayana Manickavasagam: writing – original draft, experimental work and data analysis. **Rohan Murugavel:** experimentation and data analysis. **Anubala Singaravelu Kumar:** experimentation and data analysis. **Nitin Muralidharan:** conceptualization, analysis and editing.

Acknowledgments

The authors acknowledge all the members of the EMERGE Research Group at IIT Madras, India, for their meaningful discussions and support throughout the work. This work was supported in part by the ANRF Early Career Research Grant, File No: ANRF/ECRG/2024/002205/ENS and the CSR Fund from HSBC India through Project Number CR24251368CHHSBC008836, IIT Madras for the Centre for Resource Efficiency, Recyclability and Circularity in Energy Transition, IIT Madras, Chennai-600036, Tamil Nadu, India.

Funding

Anusandhan National Research Foundation, ANRF/ECRG/2024/002205/ENS. HSBC India Limited, CR24251368CHHSBC008836.

Conflicts of Interest

The authors declare no conflicts of interest.

References

1. M. A. Hannan, S. B. Wali, P. J. Ker, et al., "Battery Energy-Storage System: A Review of Technologies, Optimization Objectives, Constraints, Approaches, and Outstanding Issues," *Journal of Energy Storage* 42 (2021): 103023.

2. U. Datta, A. Kalam, and J. Shi, "A Review of Key Functionalities of Battery Energy Storage System in Renewable Energy Integrated Power Systems," *Energy Storage* 3 (2021): e224.

3. M. Li, J. Lu, Z. Chen, and K. Amine, "30 Years of Lithium-Ion Batteries," *Advanced Materials* 30 (2018): 1800561.

4. Y. Wang, T. Yu, J. Chen, B. Gao, M. Yu, and J. Zhu, "Advances in Safety of Lithium-Ion Batteries for Energy Storage: Hazard Characteristics and Active Suppression Techniques," *Energy Reviews* 4 (2025): 100117.

5. N. Muralidharan, E. C. Self, M. Dixit, et al., "Next-Generation Cobalt-Free Cathodes – A Prospective Solution to the Battery Industry's Cobalt Problem," *Advanced Energy Materials* 12 (2022): 2103050.

6. M. Dixit, B. Witherspoon, N. Muralidharan, et al., "Insights Into the Critical Materials Supply Chain of the Battery Market for Enhanced Energy Security," *ACS Energy Letters* 9 (2024): 3780–3789.

7. J. Liu, J. Xiao, J. Yang, et al., "The TWh Challenge: Next Generation Batteries for Energy Storage and Electric Vehicles," *Next Energy* 1 (2023): 100015.

8. Y. Tian, G. Zeng, A. Rutt, et al., "Promises and Challenges of Next-Generation "Beyond Li-Ion" Batteries for Electric Vehicles and Grid Decarbonization," *Chemical Reviews* 121 (2021): 1623–1669.

9. H. Au, M. Crespo-Ribadeneyra, and M.-M. Titirici, "Beyond Li-Ion Batteries: Performance, Materials Diversification, and Sustainability," *One Earth* 5 (2022): 207–211.

10. S. T. Senthilkumar, W. Go, J. Han, et al., "Emergence of Rechargeable Seawater Batteries," *Journal of Materials Chemistry A* 7 (2019): 22803–22825.

11. S. Arnold, L. Wang, and V. Presser, "Dual-Use of Seawater Batteries for Energy Storage and Water Desalination," *Small* 18 (2022): 2107913.

12. K. Singh, A. Chakraborty, R. Thirupathi, and S. Omar, "Recent Advances in NASICON-Type Oxide Electrolytes for Solid-State Sodium-Ion Rechargeable Batteries," *Ionics* 28 (2022): 5289–5319.

13. A. Parejiya, R. Essehli, R. Amin, et al., "$Na_{1+x}Mn_{x/2}Zr_{2-x/2}(PO_4)_3$ as a Li^+ and Na^+ Super Ion Conductor for Solid-State Batteries," *ACS Energy Letters* 6 (2021): 429–436.

14. Y. Kim, H. Kim, S. Park, I. Seo, and Y. Kim, "Na Ion- Conducting Ceramic as Solid Electrolyte for Rechargeable Seawater Batteries," *Electrochimica Acta* 191 (2016): 1–7.

15. C. Lee, T.-U. Wi, W. Go, et al., "Unveiling Interfacial Dynamics and Structural Degradation of Solid Electrolytes in A Seawater Battery System," *Journal of Materials Chemistry A* 8 (2020): 21804–21811.

16. M. Li, M. Dixit, R. Essehli, et al., "$Na_3Zr_2Si_2PO_{12}$ Solid Electrolyte Membrane for High-Performance Seawater Battery," *Advanced Science* 10 (2023): 2300920.

17. J. Kim, S. Lee, S. Kim, et al., "Anode-less Hybrid Na–CO_2 Battery With Sodium Harvesting From Seawater for Both Electricity Storage and Various Chemical Production," *ACS Energy Letters* 8 (2023): 5079–5087.

18. Y. Kim, M. Künzel, D. Steinle, et al., "Anode-Less Seawater Batteries With a Na-Ion Conducting Solid-Polymer Electrolyte for Power to Metal and Metal to Power Energy Storage," *Energy & Environmental Science* 15 (2022): 2610–2618.

19. D. Mladenović, A. Mladenović, D. M. F. Santos, et al., "Transition Metal Oxides for Bifunctional ORR/OER Electrocatalysis in Unitized Regenerative Fuel Cells," *Journal of Electroanalytical Chemistry* 946 (2023): 117709.

20. Y. Tian, L. Xu, J. Qiu, X. Liu, and S. Zhang, "Rational Design of Sustainable Transition Metal-Based Bifunctional Electrocatalysts for Oxygen Reduction and Evolution Reactions," *Sustainable Materials and Technologies* 25 (2020): e00204.

21. J. Wang, H. Kong, H. Zhong, et al., "Recent Progress on Transition Metal Based Layered Double Hydroxides Tailored for Oxygen Electrode Reactions," *Catalysts* 11 (2021): 1394.

22. Y. Wang, M. Zhang, Y. Liu, et al., "Recent Advances on Transition-Metal-Based Layered Double Hydroxides Nanosheets for Electrocatalytic Energy Conversion," *Advanced Science* 10 (2023): 2207519.

23. L. Zhou, S. Jiang, Y. Liu, M. Shao, M. Wei, and X. Duan, "Ultrathin CoNiP@Layered Double Hydroxides Core–Shell Nanosheets Arrays for Largely Enhanced Overall Water Splitting," *ACS Applied Energy Materials* 1 (2018): 623–631.

24. D. Liu, B. Xue, and F. Li, "Optimization of Hydrothermal Parameters and Multifunctional Catalytic Activity of NiFe-LDH Electrocatalyst," *International Journal of Hydrogen Energy* 143 (2025): 44–58.

25. J. Long, J. Zhang, X. Xu, and F. Wang, "Crystalline NiFe Layered Double Hydroxide With Large Pore Volume as Oxygen Evolution Electrocatalysts," *Materials Chemistry and Physics* 254 (2020): 123496.

26. T. Zhan, Y. Zhang, X. Liu, S. S. Lu, and W. Hou, "NiFe Layered Double Hydroxide/Reduced Graphene Oxide Nanohybrid as an Efficient Bifunctional Electrocatalyst for Oxygen Evolution and Reduction Reactions," *Journal of Power Sources* 333 (2016): 53–60.

27. T. Kumar, B. Devi, A. Halder, and R. R. Koner, "NiFe-Coordination Polymers-Derived Layered Double Hydroxides as Bifunctional Materials: Effect of the Ni: Fe Ratio on the Electrochemical Performance," *ChemPlusChem* 88, 2023, e202300186.

28. X. Li, S.-l. Xu, J. Li, et al., "NiFe-LDH as a Bifunctional Electrocatalyst for Efficient Water and Seawater Electrolysis: Enhanced Oxygen Evolution and Hydrogen Evolution Reactions," *Nanoscale Advances* 7 (2025): 5546–5560.

29. Y. Liu, H. Hu, K. Wang, J. Huang, and D. Wang, "Advancing Seawater Electrolysis: NiFe-LDH-Based Electrocatalysts for the Oxygen Evolution Reaction," *Advanced Energy Materials* n/a (2025): e04101.

30. X. Feng, X. Hao, X. Zhao, et al., "Tailoring Nanostructured NiFe-LDH Catalysts via Ammonium Fluoride-Mediated Hydrothermal Synthesis: Enhanced Electrocatalytic Performance in Oxygen Evolution Reactions," *CrystEngComm* 27 (2025): 1483–1490.

31. H. Wang, L. Yao, H. Chen, et al., "Durable Alkaline Seawater Oxidation Over Hierarchical NiNH@NiFe LDH Nanoarrays," *Inorganic Chemistry* 64 (2025): 23108–23114.

32. D. Chauhan, M. Itagi, and Y.-H. Ahn, "Seawater Electrolysis Incorporating NiHf-LDH/MXene/NF High-Performance Electrocatalysts," *International Journal of Hydrogen Energy* 198 (2026): 152735.

33. Y. Li, Y. Wu, M. Yuan, et al., "Operando Spectroscopies Unveil Interfacial FeOOH Induced Highly Reactive β-Ni(Fe)OOH for Efficient Oxygen Evolution," *Applied Catalysis B: Environmental* 318 (2022): 121825.

34. C. Zhang, J. V. García-Meza, and Y. Li, "Differential Removal of Tetracycline Hydrochloride and Quinolone Antibiotics by Calcined and Uncalcined Layered Double Hydroxides," *Minerals and Mineral Materials* 2 (2023): 3.

35. J. H. Ryu, J. Park, J. Park, et al., "Carbothermal Shock-Induced Bifunctional Pt-Co Alloy Electrocatalysts for High-Performance Seawater Batteries," *Energy Storage Materials* 45 (2022): 281–290.

36. P. P. Machado Pico, J. Montero, A. Tsurumaki, S. Passerini, and M. A. Navarra, "Bifunctional PGM-Free Electrocatalysts for Seawater Batteries," *Sustainable Energy & Fuels* 10 (2026): 227–235.

37. L. Lu, Y. Zheng, R. Yang, A. Kakimov, and X. Li, "Recent Advances of Layered Double Hydroxides–Based Bifunctional Electrocatalysts for ORR and OER," *Materials Today Chemistry* 21 (2021): 100488.

38. L. Qian, Z. Lu, T. Xu, et al., "Trinary Layered Double Hydroxides as High-Performance Bifunctional Materials for Oxygen Electrocatalysis," *Advanced Energy Materials* 5 (2015): 1500245.

39. J. H. Hong, I. Song, Y. Cho, et al., "N-doped Carbonized Lignin for Electrocatalysts in Seawater Batteries," *Chemical Engineering Journal* 505 (2025): 159219.

40. S. Kim, J. Shim, M. Son, S. Park, and K. H. Cho, "Influence of Organic Matter on Seawater Battery Desalination Performance," *Desalination* 568 (2023): 117024.

41. S. Muthukumaran, K. Yang, A. Seuren, et al., "The Use of Ultrasonic Cleaning for Ultrafiltration Membranes in the Dairy Industry," *Separation and Purification Technology* 39 (2004): 99–107.

42. H. Cho, J. Choi, Y. Choi, and S. Lee, "Ultrasonic-Assisted Removal of Inorganic Scales in High-Salinity Wastewater Treatment using Membrane Distillation," *Desalination and Water Treatment* 157 (2019): 383–392.

Supporting Information

Additional supporting information can be found online in the Supporting Information section.